Available online at www.sciencedirect.com

ScienceDirect

Nuclear Physics B Proceedings Supplement 00 (2014) 1–4

Nuclear Physics B Proceedings Supplement

Solar neutrinos in Super-Kamioaknde

Hiroyuki Sekiya

Kamioka Observatory, Institute for Cosmic Ray Research, University of Tokyo, 456, Higashi-Mozumi, Kamioka, Hida, Gifu, 506-1205, Japan

Abstract

Recently the concern with the effect of matter on the neutrino oscillation has been growing, because the possibility of mass hierarchy determination by next generation experiments through the matter effect has been recognized. We report an indication that the elastic scattering rate of solar ^{8}B neutrinos with electrons in the Super-Kamiokande detector is larger when the neutrinos pass through Earth during nighttime. This is the first direct indication that neutrino oscillation probabilities are modified by the presence of matter. The observed the day-night asymmetry is $-3.3 \pm 1.0(stat.) \pm 0.5(syst.)$ for $\Delta m^2_{21} = 4.84 \times 10^5 \mathrm{eV}^2$, $\sin^2\theta_{12} = 0.311$ and $\sin^2\theta_{13} = 0.025$, which deviates from zero by 3σ. Since the elastic scattering process is mostly sensitive to electron-flavored solar neutrinos, a nonzero day-night asymmetry implies that the flavor oscillations of solar neutrinos are affected by the presence of matter within the neutrinos' flight path. Super-Kamiokande's day-night asymmetry is consistent with neutrino oscillations for $4 \times 10^{-5}\mathrm{eV}^2 \leq \Delta m^2_{21} \leq 7 \times 10^{-5}\mathrm{eV}^2$ and large mixing values of θ_{12} at the 68% C.L. We also report the measured recoil electron spectrum whose shape should reflect the transition between vacuum dominated oscillations (lower energy solar neutrinos) and matter dominated oscillations (higher energy solar neutrinos).

Keywords: ^{8}B neutrino, day-night asymmetry, MSW effect

1. Introduction

Solar neutrino flux measurements from Super-Kamiokande (SK) [1] and the Sudbury Neutrino Observatory(SNO) [2] have provided direct evidence for solar neutrino flavor conversion. However, there is still no clear evidence that this solar neutrino flavor conversion is indeed due to neutrino oscillations and not caused by any other mechanism. Currently there are two testable signatures unique to neutrino oscillations. The first is the observation and precision test of the MSW resonance curve [3]. Based on oscillation parameters extracted from solar neutrino and reactor anti-neutrino measurements, there is an expected characteristic energy dependence of the flavor conversion. The higher energy solar neutrinos (higher energy ^{8}B and hep neutrinos) undergo complete resonant conversion within the sun, while the flavor changes of the lower energy solar neutrinos (pp, ^{7}Be, pep, CNO and lower energy ^{8}B neutrinos) arise only from vacuum oscillations, which limits the average electron flavor survival probability to exceed 50%. The transition from the matter dominated oscillations within the sun, to the vacuum dominated oscillations, should occur near 3 MeV, making ^{8}B neutrinos the best choice when looking for a transition point within the energy spectrum. A second signature unique to oscillations arises from the effect of the terrestrial matter density on solar neutrino oscillations. This effect is tested directly by comparing solar neutrinos which pass through the Earth at nighttime to those which do not during the daytime. Those neutrinos which pass through the Earth will in general have an enhanced electron neutrino content compared to those which do not, leading to an increase in the nighttime electron elastic scattering rate (or any charged-current interaction rate), and hence a negative “day/night asymmetry”. SK de-

Email address: sekiya@icrr.u-tokyo.ac.jp (Hiroyuki Sekiya)

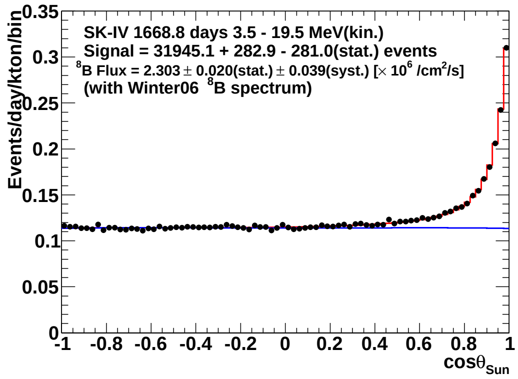

Figure 1: Solar angle distribution for 3.5-19.5 MeV. θ_{sun} is the angle between the incoming neutrino direction and the reconstructed recoil electron direction. Black points are data while the blue and red histograms are best fits to the background and signal plus background, respectively.

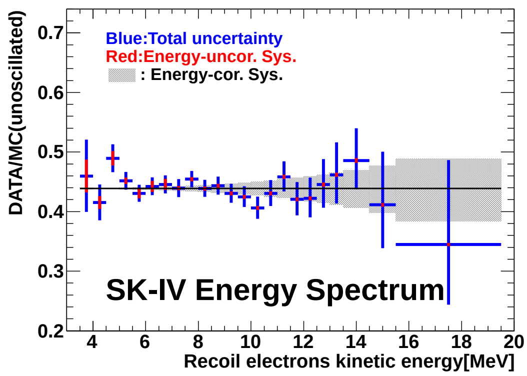

Figure 2: SK-IV energy spectrum. The horizontal dashed line gives the SK-IV average. Error bars shown are statistical plus energy-uncorrelated systematic uncertainties. Energy-correlated systematic uncertainties are shown separately as shaded region.

tects ^{8}B solar neutrinos over a wide energy range in real time, making it a prime detector to search for both solar neutrino oscillation signatures.

2. Results with new SK-IV data

The start of physics data taking of SK-IV occurred on October 6th, 2008, with this report including data taken until January 31st, 2014. The total livetime is 1668.8 days. The entire data period was taken using the same low energy threshold, with about 85% triggering efficiency at 3.5-4.0 MeV kinetic energy, 99% at 4.0-4.5 MeV kinetic energy and 100% above 4.5 MeV kinetic energy.

In the case of ν-e interactions of solar neutrinos in SK, the incident neutrino and recoil electron directions are highly correlated. Fig.1 shows the $\cos\theta_{\text{sun}}$ distribution for events between 3.5-19.5 MeV. In order to obtain the number of solar neutrino interactions, an extended maximum likelihood fit is used. This method is also used in the SK-I [1], II [4], and III [5] analyses. The red line of Fig.1 is the best fit to the data. The blue line shows the background component of that best fit.

The combined systematic uncertainty of the total flux in SK-IV is found to be 1.7% as the quadratic sum of all components. This is the best value seen throughout all phases of SK, much improved over 2.2% in SK-III. The main contributions to the reduction come from improvements in the uncertainties arising from the energy-correlated uncertainties (energy scale and resolution), the vertex shift, trigger efficiency and the angular resolution. SK-III data below 6.0 MeV recoil electron kinetic energy has only about half the livetime as the data above, while SK-IV's livetime is the same for all energy bins. As a consequence, the energy scale and resolution uncertainties lead to a smaller systematic uncertainty of the flux in SK-IV than in SK-III. The higher efficiency of SK-IV between 5.0 and 6.0 MeV (kinetic) of SK-IV and the addition of the 3.5 to 4.5 MeV data lessens the impact of energy scale and resolution uncertainty on the flux determination even further. The number of solar neutrino events (between 3.5 and 19.5 MeV) is $31,945^{+283}_{-281}$(stat.) ± 543(syst.). This number corresponds to a ^{8}B solar neutrino flux of $\Phi_{^8B} = (2.303 \pm 0.020(\text{stat.}) \pm 0.039(\text{syst.})) \times 10^6/(\text{cm}^2\text{sec})$, assuming a pure ν_e flavor content.

Fig.2 shows the resulting SK-IV energy spectrum. SK-IV has $N_{\text{bin}} = 23$ energy bins; 20 bins of 0.5 MeV width between 3.5-13.5 MeV, two energy bins of 1 MeV between 13.5 and 15.5 MeV, and one bin between 15.5 and 19.5 MeV.

To test the expected "upturn" below ~6 MeV from the MSW resonance effects, the best fit oscillation parameters of solar experiments and solar + KamLAND (described later) were fitted to all the SK-I to SK-IV spectra, and it is disfavored by 1σ and 1.7σ respectively so far. Fitted results are shown in Fig.3.

The SK-IV livetime during the day (night) is 799.7 days (869.1 days). The solar neutrino flux between 4.5 and 19.5 MeV and assuming no oscillations is measured as $\Phi_D = (2.25 \pm 0.03(\text{stat.}) \pm 0.38(\text{sys.})) \times 10^6/(\text{cm}^2\text{sec})$ during the day and $\Phi_N = (2.36 \pm 0.03(\text{stat.}) \pm 0.40(\text{sys.})) \times 10^6/(\text{cm}^2\text{sec})$ during the night. A more sophisticated method to test the day/night effect is given in [1, 6]. For a given set of oscillation parameters, the interaction rate as a function of the so-

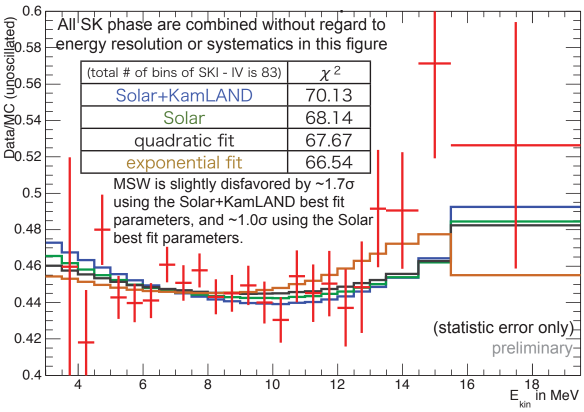

Figure 3: All SK phase combined energy spectrum and fitted functions.

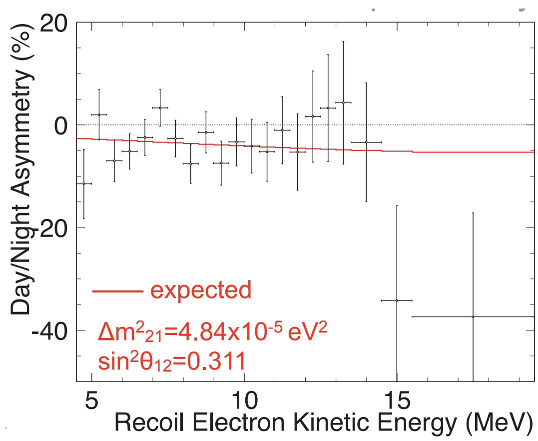

Figure 4: SK combined energy dependence of the fitted day/night asymmetry (measured day/night amplitude times the expected asymmetry (red)) for $\Delta m^2_{21} = 4.84 \times 10^{-5}$eV^2, $\sin^2\theta_{12} = 0.311$ and $\sin^2\theta_{13} = 0.025$. The error bars shown are statistical uncertainties only.

lar zenith angle is predicted. Only the shape of the calculated solar zenith angle variation is used, the amplitude of it is scaled by an arbitrary parameter. The extended maximum likelihood fit to extract the solar neutrino signal is expanded to allow time-varying signals. The likelihood is then evaluated as a function of the average signal rates, the background rates and the scaling parameter which is called the "day/night amplitude". The equivalent day/night asymmetry is calculated by multiplying the fit scaling parameter with the expected day/night asymmetry. In this manner the day/night asymmetry is measured more precisely statistically. Because the amplitude fit depends on the assumed shape of the day/night variation, it necessarily depends on the oscillation parameters, although with very little dependence expected on the mixing angles (in or near the large mixing angle solutions and for θ_{13} values consistent with reactor neutrino measurements [7]).

The day/night asymmetry coming from the SK-I to IV combined amplitude fit can be seen as a function of recoil electron kinetic energy in Fig.4, for $\Delta m^2_{21} = 4.84 \times 10^5$eV^2, $\sin^2\theta_{12} = 0.311$ and $\sin^2\theta_{13} = 0.025$. The day/night asymmetry in this figure is found by multiplying the fitted day/night amplitude from each energy bin, to the expected day/night asymmetry (red distribution) from the corresponding bin.

Fig.5 shows the Δm^2_{21} dependence of the SK all phases combined day/night asymmetry for $\sin^2\theta_{12} = 0.311$ and $\sin^2\theta_{13} = 0.025$. Here the day/night asymmetry is also found by multiplying the fitted day/night amplitude by the expected day/night asymmetry (red curve). The point where the best fit crosses the expected curve represents the value of Δm^2_{21} where the measured day/night asymmetry is equal to the expectation. Superimposed are the allowed ranges in Δm^2_{21} from the global solar neutrino data fit (green) and from KamLAND (blue). The amplitude fit shows no dependence on the values of θ_{12} (within the LMA region of the MSW plane) or θ_{13}.

3. Oscillation analysis

We analyzed the SK-IV elastic scattering rate, the recoil electron spectral shape and the day/night variation to constrain the solar neutrino oscillation parameters. We then combined the SK-IV constraints with those of previous SK phases, as well as other solar neutrino experiments. The allowed contours of all solar neutrino data (as well as KamLAND's constraints) are shown in Fig.6 and 7. In Fig.6 the contours from the fit to all solar neutrino data are almost identical to the ones of the SK+SNO combined fit. In the right panel some tension between the solar neutrino and reactor anti-neutrino measurements of the solar Δm^2_{21} is evident. This tension is mostly due to the SK day/night measurement. Even though the expected amplitude agrees well within 1σ with the fitted amplitude for any Δm^2_{21} in either the KamLAND or the SK range, the SK data somewhat favor the shape of the variation predicted by values of Δm^2_{21} that are smaller than KamLAND's. The best fit values are $\sin^2\theta_{12} = 0.308 \pm 0.013$, $\Delta m^2_{21} = 7.50^{+0.19}_{-0.18} \times 10^{-5}$eV^2, and $\sin^2\theta_{13} = 0.027^{+0.016}_{-0.014}$. The significance of non-zero θ_{13} is about 2σ.

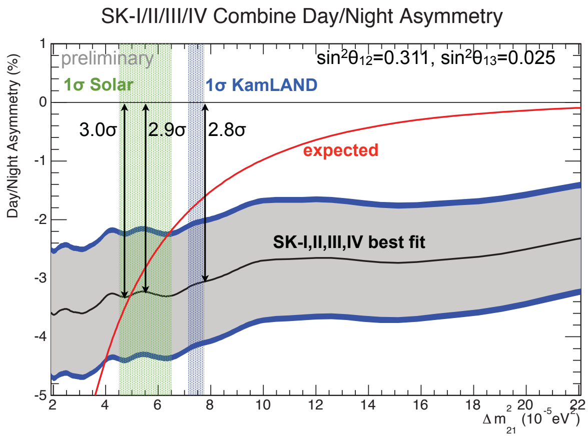

Figure 5: Dependence of the measured day/night asymmetry (fitted day/night amplitude times the expected day/night asymmetry (red)) on Δm^2_{21} (light gray band=stat. error, dark gray band=stat.+syst. error) for $\sin^2\theta_{12} = 0.311$ and $\sin^2\theta_{13} = 0.025$. Overlaid are the allowed ranges from solar neutrino data (green band) and KamLAND (blue band).

4. Summary

In summary, the analysis threshold was successfully lowered to 3.5 MeV kinetic recoil electron energy in SK-IV and by adding SK-IV data, ~70,000 solar neutrino interactions has been observed in ~4,500 days, by far the largest sample of solar neutrino events in the world. SK spectrum results slightly disfavor the MSW resonance curves, but are consistent with MSW prediction within $1 \sim 1.7\sigma$. SK data provide the first indication (at $2.8 \sim 3.0\sigma$) of terrestrial matter effects on ^{8}B solar neutrino oscillation. This is the first observation using a single detector and identical neutrino beams that matter affects neutrino oscillations [8]. These SK measurements strongly constrain neutrino oscillation parameters: SK uniquely selects the Large Mixing Angle MSW region by $> 3\sigma$, gives world's best constraint on Δm^2_{21} using neutrinos, and significantly contributes to the measurement of θ_{12}.

References

[1] J.Hosaka et al., Phys. Rev. D73, 112001 (2006).
[2] Q.R.Ahmad et al., Phys. Rev. Lett. 87 071301 (2001).
[3] S.P.Mikheyev and A.Y.Smirnov, Sov. Jour. Nucl. Phys. 42, 913 (1985); L.Wolfenstein, Phys. Rev. D17, 2369 (1978).
[4] J.P.Cravens et al., Phys. Rev. D 78, 032002(2008).
[5] K.Abe et al., Phys. Rev. D 83 052010 (2011).
[6] M.B.Smy et al., Phys. Rev. D. 69, 011104(R) (2004).
[7] F.P.An et al., arXiv:1210.6327 (2012); J.K.Ahn et al., Phys.Rev.Lett. 108 191802 (2012); Y.Abe et al.,Phys.Rev. D86 052008 (2012).
[8] A.Renshaw et al., Phys. Rev. Lett. 112, 091805 (2014).

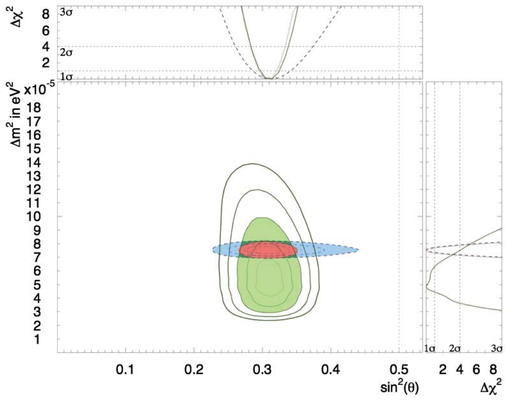

Figure 6: Allowed contours of Δm^2_{21} vs. $\sin^2\theta_{12}$ from solar neutrino data (green) at 1, 2, 3, 4 and 5 σ and Kam-LAND data (blue) at the 1, 2 and 3 σ confidence levels. Also shown are the combined results in red. For comparison, the almost identical results of the SK+SNO combined fit are shown by the dashed dotted lines. θ_{13} is constrained by $\sin^2\theta_{13} = 0.0242 \pm 0.0026$.

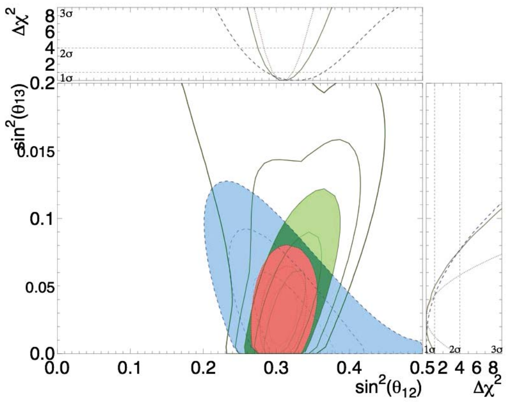

Figure 7: Allowed contours of $\sin^2\theta_{13}$ vs. $\sin^2\theta_{12}$ from solar neutrino data (green) at 1, 2, 3, 4 and 5 σ and KamLAND measurements (blue) at the 1, 2 and 3 σ confidence levels. Also shown are the combined results in red.